

Cosmic viscosity as a remedy for tension between PLANCK and LSS data

Sampurn Anand,^a Prakrut Chaubal,^a Arindam Mazumdar,^a
Subhendra Mohanty^a

^aPhysical Research Laboratory, Ahmedabad, 380009, India

E-mail: sampurn@prl.res.in, prakrutchaubal@gmail.com, arindam@prl.res.in,
mohanty@prl.res.in

Abstract. Measurements of σ_8 from large scale structure observations show a discordance with the extrapolated σ_8 from Planck CMB parameters using Λ CDM cosmology. Similar discordance is found in the value of H_0 and Ω_m . In this paper, we show that the presence of viscosity, shear or bulk or combination of both, can remove the above mentioned conflicts simultaneously. This indicates that the data from Planck CMB observation and different LSS observations prefer small but non-zero amount of viscosity in cold dark matter fluid.

Keywords: self interacting dark matter, shear viscosity, large scale structures, CMB

Contents

1	Introduction	1
2	Effect of viscosity on large scale structures	2
2.1	Perturbation equations	3
2.2	Growth factor and effect on matter power spectrum	5
3	Resolving σ_8-Ω_m tension	8
4	Resolving H_0-Ω_m tension	9
5	Planck-LSS combined viscous-cosmological parameters	10
6	Discussion and Conclusion	11

1 Introduction

Over the past few decades, several observations have indicated that our Universe is dominated by dark components, namely, dark matter (DM) and Dark energy (DE) [1–8]. In the light of current observations from Cosmic Microwave Background (CMB) and Large Scale Structure (LSS) observations, most favorable theoretical construct to understand the evolution of our Universe is provided by the Cold Dark Matter with cosmological constant, Λ , also referred as the *standard model of cosmology* (Λ CDM model), which is characterized by six parameters only. Predictions of Λ CDM cosmology have been seen successfully in the CMB observations. However, LSS observations have shown some conflicts with it. In this paper we will address these issues and will ameliorate these conflicts by introducing dissipative effects in the system.

The standard six parameters of Λ CDM model are : the ratio of density of cold dark matter and baryonic matter to the critical density, Ω_{cdm}^0 and Ω_b^0 respectively, evaluated today, the acoustic scale Θ_{MC} , the amplitude (A_s) and the spectral index (n_s) of the primordial density perturbations and the optical depth to the epoch of reionization (τ_{reion}). The value of Hubble parameter at current epoch H_0 is related to the acoustic scale, Θ_{MC} . As a consequence, one of them is considered as input model parameter leaving other as a derived quantity. These parameters are inferred from two different observations namely CMB and LSS. This type of indirect determination has mostly provided the value of H_0 lower than the direct measurement from type-IA supernova [9]. However, before the release of Planck data [7] the inferred value of H_0 from CMB was in agreement with that of the LSS observations.

The success of Λ CDM model lies in its capability of describing the observed quantities in large scales and small scales in a single theoretical framework. The primary CMB anisotropies provide an estimate of the amplitude of the matter fluctuations at the last scattering surface. Given a cosmological model, these primary fluctuations can be extrapolated to provide an estimate of matter fluctuations at a later time in the Universe. However, the above described framework for Λ CDM model predicts the value of σ_8 , r.m.s fluctuation of perturbations at $8h^{-1}$ Mpc scale, which is not agreement with other low-redshift observations of large-scale structure [10–16]. These disagreements in the value of H_0 and σ_8 inferred from CMB and LSS observations are typically attributed either to the signals of new physics or to the systematic

errors. The recent result from dark energy survey has also shown the similar tension in $\sigma_8 - \Omega_m^0$ plane [8, 17], which indicates some new physics might be responsible for this mismatch.

Several attempts have been made in this regard to address this discordance between CMB and LSS observations. It has been argued that the interaction between dark matter and dark energy [18–20] as well as dark matter and dark radiation [21–23] can resolve this tension to some extent. However, in most of the cases such models resolve one of the above mentioned tensions but fails to solve the other one. More importantly, interaction between the dark sectors can also modify the scale corresponding to matter radiation equality [20] which might introduce greater problem than σ_8 mismatch. Some other attempts have been made by modifying the neutrino sector [24–26]. Addition of massive sterile neutrino in the system has been reported to reduce some tension in $\sigma_8 - \Omega_m^0$ plane but not in $H_0 - \Omega_m^0$ plane [24, 25]. Recently, it has been claimed that quartessence models, where a single dark component mimics both dark matter and dark energy can reduce the tension in $\sigma_8 - \Omega_m^0$ [27].

It has been discussed that the viscosity in CDM has the ability of reducing power on the small length scales [28–30]. The effect of bulk has been investigated extensively in [29]. On the other hand, the effect of shear has also been investigated to some extent [31]. Attempts to quantify the dissipative effects in dark matter has been done in ref. [32] from Baryon Acoustic Oscillation (BAO) data. For recent review on this topic, refer to [33]. The bulk viscosity suppresses the growth of structures by imparting a negative pressure against the gravitational collapse while the shear viscosity reduces the amount of velocity perturbations which in turn stops the growth. Therefore, on the small length scales, where the homogeneity and isotropy are broken due to velocity gradients, effects of shear viscosity is expected to play crucial role. Although the physics of these viscosities are different, we will show that there effect on large scale structure is more or less similar.

This paper is organized as follows: in section 2, we discuss the basic setup of viscous cosmology. This section is divided into two subsections 2.1 and 2.2. In 2.1 we outline the cosmological perturbation theory and derive the perturbation equations in presence of the two viscosities. Further, in 2.2 we show the effect of these viscosities on the growth of density perturbations which in turn effects the matter power spectrum. Having discussed the effects on the matter power spectrum, we move on to perform Markov-Chain-Monte-Carlo (MCMC) analysis with data from different CMB and LSS observations. In section 3, we show that the inclusion of viscosities removes the tension between the Planck and LSS data in $\sigma_8 - \Omega_m^0$ plane. Similarly, in section 4 we show the concordance between Planck and LSS data in $H_0 - \Omega_m^0$ plane due to viscosities. We also perform a joint analysis of Planck and LSS data with viscosities to infer the parameters of viscous cosmology in section 5. Finally, we conclude and discuss our results in section 6.

2 Effect of viscosity on large scale structures

Cosmological perturbations have been computed with the assumption of homogeneity and isotropy on large scale in presence of an ideal fluid [34–37]. Although violation of these symmetries might be prominent on small length scales, their effect might not be substantial on large scales. The reason behind it is that velocity gradient on smaller scales becomes significant. Therefore, we go beyond the perfect fluid approximation by considering dissipative effects in the system. In this section we will describe the cosmological perturbation theory with non-ideal fluid in the presence of shear and bulk viscosities.

The energy momentum tensor for the non-ideal fluid is given as [38]

$$T_{vf}^{\mu\nu} = \rho u^\mu u^\nu + (p + p_b) \Delta^{\mu\nu} + \pi^{\mu\nu}, \quad (2.1)$$

where ρ is the energy density and p is the pressure in the rest frame of the fluid, $p_b = -\zeta \nabla_\mu u^\mu$ is the bulk viscous pressure with bulk viscosity ζ . $\pi^{\mu\nu}$ is the shear-viscous tensor which takes the following form

$$\pi^{\mu\nu} = -2\eta \sigma^{\mu\nu} = -2\eta \left[\frac{1}{2} (\Delta^{\mu\alpha} \nabla_\alpha u^\nu + \Delta^{\nu\alpha} \nabla_\alpha u^\mu) - \frac{1}{3} \Delta^{\mu\nu} (\nabla_\alpha u^\alpha) \right], \quad (2.2)$$

with η being the shear viscosity and $\Delta^{\mu\nu} = u^\mu u^\nu + g^{\mu\nu}$ being the projection operator which projects to the subspace orthogonal to the fluid velocity. It is evident that $\pi_\mu^\mu = 0 = u_\mu \pi^{\mu\nu}$. Conservation of energy momentum, $\nabla_\nu T^{\mu\nu} = 0$, leads to the viscous fluid dynamic equations [28]

$$u^\mu \nabla_\mu \rho + (\rho + p) \nabla_\mu u^\mu - \zeta (\nabla_\mu u^\mu)^2 - 2\eta \sigma^{\mu\nu} \sigma_{\mu\nu} = 0, \quad (2.3)$$

$$(\rho + p + p_b) u^\mu (\nabla_\mu u^\alpha) + \Delta^{\alpha\mu} \nabla_\mu (p + p_b) + \Delta_\nu^\alpha \nabla_\mu \pi^{\mu\nu} = 0. \quad (2.4)$$

2.1 Perturbation equations

Perturbation in the matter field is related to the perturbation in the metric through Einstein's equation and vice-versa. In general, metric tensor $g_{\mu\nu}$ can have scalar, vector and tensor perturbations which are independent of each other in linear order. In this analysis we consider only scalar perturbations in the conformal-Newtonian gauge given as

$$ds^2 = a^2(\tau) \left[-(1 + 2\psi(\tau, \vec{x})) d\tau^2 (1 - 2\phi(\tau, \vec{x})) dx_i dx^i \right], \quad (2.5)$$

where $\psi(\tau, \vec{x})$ and $\phi(\tau, \vec{x})$ are space-time dependent functions. We assume a spatially flat universe consisting of one species of viscous CDM along with cosmological constant (Λ). Normalization of the flow field u^μ as $u_\mu u^\mu = -1$ allows us to express it in terms of coordinate velocity v^i and the metric perturbations as

$$u^\mu = \frac{1}{a\sqrt{1 + 2\psi - (1 - 2\phi)v^2}} (1, v^i) \approx \frac{1}{a} (1 - \psi, v^i) + \text{higher order terms}. \quad (2.6)$$

We parametrize the density and pressure in terms of isotropic background and spatially varying small perturbations as

$$\begin{aligned} \rho_m(\tau, \vec{x}) &= \rho_m(\tau) + \delta\rho(\tau, \vec{x}), \\ p(\tau, \vec{x}) &= p(\tau) + \delta p(\tau, \vec{x}), \end{aligned} \quad (2.7)$$

with $\delta\rho, \delta p \ll \rho_m$. The background field satisfies the following equations:

$$\mathcal{H}^2 = \left(\frac{\dot{a}}{a} \right)^2 = \frac{8\pi G}{3} (\rho_m + \Lambda) a^2, \quad (2.8)$$

$$\dot{\rho}_m + 3\mathcal{H} (\rho_m + p_m) = 0, \quad (2.9)$$

where $\mathcal{H} = \dot{a}/a$ is the Hubble parameter and dot denotes the derivative with respect to the conformal time τ . For the analysis below, we consider perturbations, up to linear order, in the variables $\delta\rho, \delta p, v^i, \phi$ and ψ .

In order to expand the fluid dynamic equations, we use the normalized density contrast $\delta = \delta\rho/\rho_m$ and the velocity divergence $\theta = \nabla_i v^i$. Moreover, δp is related to the density perturbations through w , the equation of state parameter, as

$$w = \frac{p_m}{\rho_m}, \quad c_s^2 = \frac{\delta p}{\delta\rho}, \quad c_{\text{ad}}^2 = \frac{\dot{p}_m}{\dot{\rho}_m} = w - \frac{\dot{w}}{3\mathcal{H}(1+w)}, \quad (2.10)$$

where c_s is the speed of sound in the medium and c_{ad} is the adiabatic sound speed.

Inclusion of these perturbations in eq. (2.3) and eq. (2.4) leads to the dynamical equations which govern the evolution of cosmological perturbations. In Fourier space these equations can be written as [28],

$$\dot{\delta} = -(1+w) (\theta - 3\dot{\phi}) - 3\mathcal{H} (c_s^2 - w) \delta, \quad (2.11)$$

$$\dot{\theta} = -\mathcal{H}\theta + k^2\psi + \left(\frac{c_s^2}{1+w}\right) k^2\delta + 3c_{\text{ad}}^2\mathcal{H}\theta - \frac{4}{3}k^2 \frac{\eta}{(1+w)a\rho_m} \theta. \quad (2.12)$$

For viscous matter we will evaluate the quantities defined in eq.(2.10).

Equation of state, w : For baryonic matter and CDM, pressure $p_m = 0$. However, in presence of bulk viscosity the effective pressure of CDM is equal to the bulk pressure $p_b = -\zeta \nabla_\mu u^\mu = -3\zeta \mathcal{H}/a$. Therefore, the equation of state parameter for CDM is

$$w = -\frac{3\zeta\mathcal{H}}{a\rho_{\text{cdm}}} = -\frac{\tilde{\zeta}a}{\Omega_{\text{cdm}}\tilde{\mathcal{H}}}, \quad (2.13)$$

where $\tilde{\zeta} = 8\pi G\zeta/\mathcal{H}_0$ is a dimensionless parameter and $\tilde{\mathcal{H}} = \mathcal{H}/\mathcal{H}_0$. Throughout the manuscript ‘0’ in the superscript or subscript denotes the value of the quantity evaluated today.

Sound speed, c_s^2 : Assuming a constant bulk viscosity, one can calculate

$$c_s^2 = -\frac{\zeta\theta}{a\rho_{\text{cdm}}\delta} = \frac{w\theta}{3\mathcal{H}\delta} = -\left(\frac{\tilde{\zeta}a}{\Omega_{\text{cdm}}\tilde{\mathcal{H}}}\right) \left(\frac{\theta}{3\mathcal{H}\delta}\right). \quad (2.14)$$

Adiabatic sound speed, c_{ad}^2 : Using eq.(2.13) and performing a little bit of mathematical manipulation, we obtain

$$c_{\text{ad}}^2 = 2w \left(1 - \frac{\Omega_{\text{cdm}}}{4}\right). \quad (2.15)$$

In terms of quantities defined above, the evolution equation for δ of CDM (eq. (2.11)) takes the following form

$$\dot{\delta} = -\left(1 - \frac{\tilde{\zeta}a}{\Omega_{\text{cdm}}\tilde{\mathcal{H}}}\right) (\theta - 3\dot{\phi}) + \left(\frac{\tilde{\zeta}a}{\Omega_{\text{cdm}}\tilde{\mathcal{H}}}\right) \theta - \left(\frac{3\mathcal{H}\tilde{\zeta}a}{\Omega_{\text{cdm}}}\right) \delta \quad (2.16)$$

and the evolution equation for θ of CDM (eq. (2.1)) becomes

$$\dot{\theta} = -\mathcal{H}\theta + k^2\psi - \frac{k^2 a \theta}{3\mathcal{H}(\Omega_{\text{cdm}}\tilde{\mathcal{H}} - \tilde{\zeta}a)} \left(\tilde{\zeta} + \frac{4\tilde{\eta}}{3}\right) - 6\mathcal{H}\theta \left(1 - \frac{\Omega_{\text{cdm}}}{4}\right) \left(\frac{\tilde{\zeta}a}{\Omega_{\text{cdm}}\tilde{\mathcal{H}}}\right), \quad (2.17)$$

where $\tilde{\eta} = 8\pi G\eta/\mathcal{H}_0$ is a dimensionless parameter.

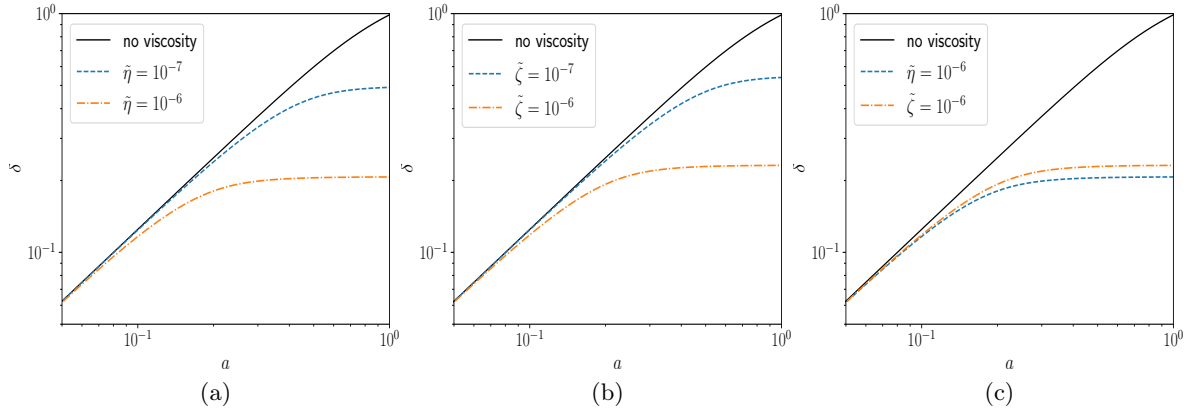


Figure 1: Effect of viscosity on the growth of linear over-density (δ) as a function of scale factor has been plotted for different values of : (a) shear (b) bulk viscosities. In figure (c) we have compared the effect of bulk and shear viscosities. We have set $k \sim 3.4 h \text{ Mpc}^{-1}$ in all the three plots.

The Poisson equation for viscous cosmology remain unchanged and given as

$$\nabla^2 \phi = 3\mathcal{H}\dot{\phi} + \frac{a^2}{2}\rho_m(\delta + 2\psi). \quad (2.18)$$

The Euler equation in Fourier space gives

$$\dot{\phi} = \frac{3a^2(p_b + \rho_m)}{k^2}\theta - \mathcal{H}\psi + \frac{\eta a}{2}(3\dot{\theta} - k^2\psi + 3\mathcal{H}\theta). \quad (2.19)$$

2.2 Growth factor and effect on matter power spectrum

It is evident from eq.(2.16) and eq.(2.17) that the growth of the overdense region gets affected by shear as well as bulk viscosity. While bulk viscosity directly slows down the collapse of the overdense region, shear viscosity imparts similar effect through the velocity perturbation. Thus, it is important to investigate the effects of these viscosities on the evolution of δ and θ which in turn effects the matter power spectrum [29, 31].

We start by considering effect of shear viscosity on the evolution of perturbations. For this purpose, we set $\tilde{\zeta} = 0$ and neglect $\dot{\phi}$. Therefore, eq. (2.16) and eq. (2.17) can be rewritten as

$$\dot{\delta} = -\theta, \quad (2.20)$$

$$\dot{\theta} = -\mathcal{H}\theta + k^2\psi - \frac{4\tilde{\eta}}{9} \frac{a\mathcal{H}_0}{\Omega_{\text{cdm}}} \frac{k^2}{\mathcal{H}^2} \theta, \quad (2.21)$$

with

$$k^2\psi = -\frac{3}{2}\Omega_{\text{cdm}}\mathcal{H}^2\delta. \quad (2.22)$$

Note that there are two dissipative terms in the right hand side of eq.(2.21), namely the Hubble expansion and the shear viscosity term. If the shear term is greater than the Hubble term then the evolution of θ is governed by shear along with the potential ψ . By comparing the

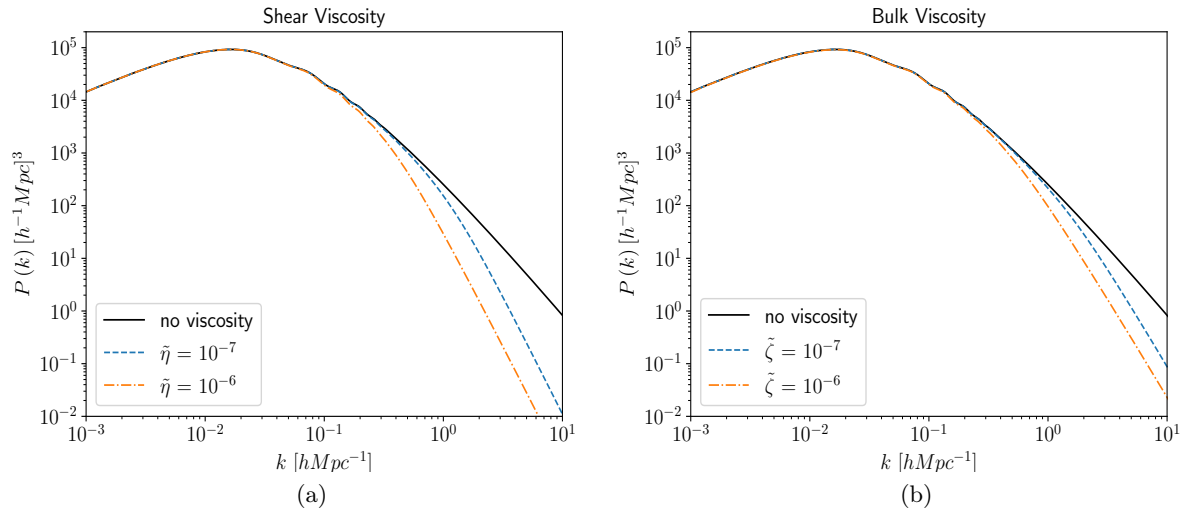


Figure 2: The effect of viscosities on the matter-power-spectrum is shown for different values of (a) shear (b) bulk viscosities. It is evident that these viscosities play important role on large k .

first and last term of eq.(2.21), we can do an order of magnitude estimate for $\tilde{\eta}$ to influence the evolution of the velocity perturbation which ultimately influences the matter power spectrum. For $a = 1$ case, $\tilde{\eta}$ turns out to be $\tilde{\eta} = \frac{9}{4} \left(\frac{k}{\mathcal{H}_0} \right)^{-2} \Omega_{\text{cdm}}^0$. For $k \sim 1 \text{Mpc}^{-1}$ the value of shear viscosity is $\tilde{\eta} \sim \mathcal{O}(10^{-8})$.

We combine the set of equations eq. (2.20) and eq. (2.21) in a single second order differential equation in terms of a as,

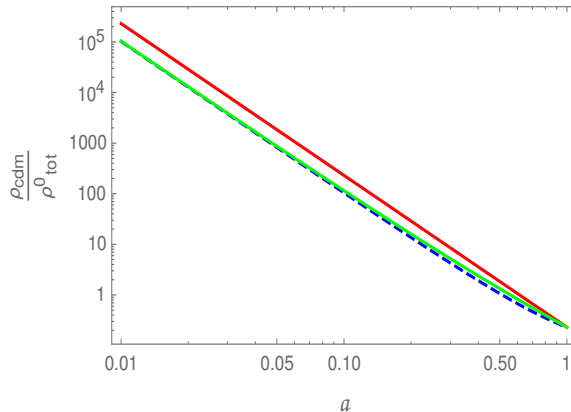
$$\delta'' + \left[\frac{2}{a} + \frac{\mathcal{H}'}{\mathcal{H}} + \frac{4}{9} \frac{k^2 \tilde{\eta} a}{\tilde{\mathcal{H}} \Omega_{\text{cdm}}^0} \right] \delta' - \frac{3}{2} \frac{\Omega_{\text{cdm}}^0}{a^3 \tilde{\mathcal{H}}^2} \delta = 0, \quad (2.23)$$

where prime represents derivative with respect to the scale factor a . Solution of this equation gives the growth of linear over density δ with a which has been plotted in Fig. (1a). For solving this equation the initial value of δ at $a = 10^{-3}$ has been set to $\frac{2}{5} \frac{a}{\Omega_m^0}$ and the value of δ' is $\frac{2}{5} \frac{a}{\Omega_m^0}$. We see in Fig. (1a) that the growth of linear overdensity gets suppressed at late time.

On the other hand, effect of bulk viscosity appears in two different ways. First, it modifies the background evolution of cold dark matter and second, it changes the perturbation-equation for δ as well as θ . Since bulk viscosity of dark matter changes the equation of state (see eq. (2.13)), the evolution ρ_{cdm} with a also gets modified which is depicted through the continuity equation (eq. (2.9)) as

$$\rho'_{\text{cdm}} + \frac{3\rho_{\text{cdm}}}{a} \left(1 - \frac{\tilde{\zeta} \rho_{\text{tot}}^0}{\rho_{\text{cdm}}} \left[\frac{\Omega_b^0}{a^3} + \Omega_\Lambda + \frac{\rho_{\text{cdm}}^0}{\rho_{\text{tot}}} \right]^{1/2} \right) = 0. \quad (2.24)$$

We solve this equation numerically and fit the solution (see Fig. (3a)), for numerical work,



(a)

Figure 3: Change in the evolution of ρ_{cdm} in the presence of bulk viscosity. The blue-dashed line shows the numerical solution of eq. (2.24) for $\tilde{\zeta} \sim 0.1$. The value of ζ has been taken too large for demonstration purpose. The green-solid line shows the fitting function given in eq. (2.25) with $\beta = 0.558$. The red-solid line represents standard $\rho_{\text{cdm}} = \frac{\rho_{\text{cdm}}^0}{a^3}$.

with a function of the following form

$$\rho_{\text{cdm}}(a) = \alpha \frac{\rho_{\text{cdm}}^0}{a^3} + \beta \frac{\rho_{\text{cdm}}^0}{a^2}, \quad (2.25)$$

where normalization at $a = 1$ ensures that $\alpha = 1 - \beta$. We have verified that this form fits well even for large range of $\tilde{\zeta}$. This form of $\rho_{\text{cdm}}(a)$ will be used in numerical solution using CLASS [39, 40] later in the paper. The value of β for $\tilde{\zeta} = 10^{-6}$ turns out to be 6.18×10^{-6} .

To consider the effect of bulk on the perturbation equations, we set $\tilde{\eta} = 0$ in equations (eq. (2.16) and eq. (2.17)) and solve them numerically. The solution is plotted and shown in Fig. (1b). Therefore, we can see that bulk viscosity has similar effect as that of the shear viscosity. However, the effect of shear viscosity is slightly more than that of the bulk viscosity on the growth of delta as shown in Fig. (1c).

The suppression of δ at late time due to viscosities shows its effect on matter power spectrum. We have seen in eq. (2.17) that the bulk and shear viscosities come into the equation multiplied with a k^2 factor. Therefore on small length scales their effects become prominent. This is expected as the velocity gradients are more effective on small length scales resulting in large viscosity and hence suppressing the growth at those scales. Consequently, one would expect that the shear viscosity may influence σ_8 . To get the matter power-spectrum we have used publicly available CLASS code [39, 40]. We have not used non-linear halo-fit for evolution of δ at large k , since non-linear evolution of viscous dark-matter is beyond the scope of this paper. We will use this power spectrum to get the value of σ_8 which corresponds to $k \sim 0.78 h \text{ MPc}^{-1}$, the scale which is expected not to be effected by non-linearities. The power-spectrum has been plotted in Fig. (2a) and Fig. (2b) where we can see as expected the larger k modes of δ gets more suppressed. In these figures we have extended the linear analysis beyond $k = 1 h \text{ MPc}^{-1}$ only for the purpose of demonstration.

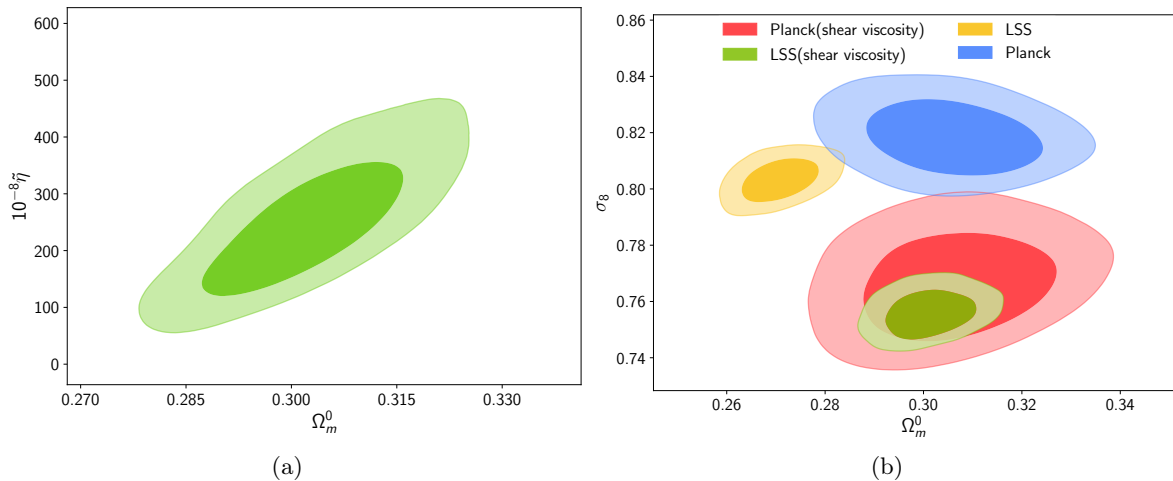


Figure 4: (a) The best-fitted range of $\tilde{\eta}$ with 1- σ and 2- σ contour for LSS data (Planck SZ + lensing, BAO-BOSS, SPT and CFHTLenS) is shown. The central value of best fit is 2.30×10^{-6} . (b) We show the Planck (high- ℓ + low - ℓ) and LSS fitted region of $\sigma_8 - \Omega_m^0$ which clearly shows the discordance. The discordance ends when the best-fit value of shear viscosity is used.

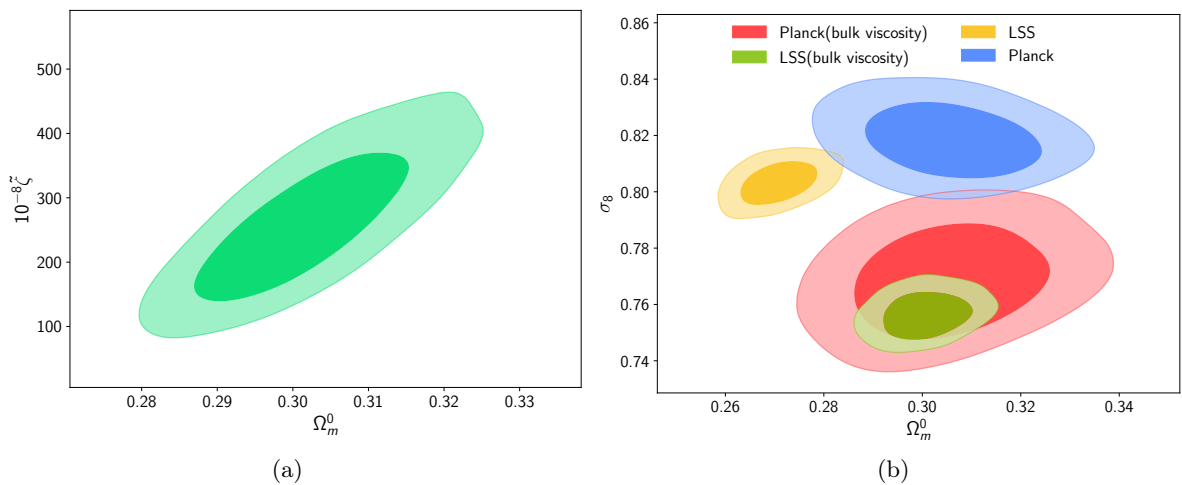


Figure 5: (a) The best-fitted range of $\tilde{\zeta}$ with 1- σ and 2- σ contour for LSS data (Planck SZ + lensing, BAO-BOSS, SPT and CFHTLenS) is shown. The central value of best fit is 2.60×10^{-6} . (b) We show the Planck (high- ℓ + low - ℓ) and LSS fitted region of $\sigma_8 - \Omega_m^0$ which clearly shows the discordance. The discordance ends when the best-fit value of bulk viscosity is used.

3 Resolving $\sigma_8 - \Omega_m$ tension

In this section we will show that there exist some tension between the LSS observations and Planck CMB observation in $\sigma_8 - \Omega_m^0$ plane. We will also demonstrate that small but non-zero amount of viscosity in cold-dark matter can remove this tension.

In order to quantify our analysis we proceed in four steps. First, we find the best-fit values of σ_8 and other cosmological parameters without viscosity from Planck high- ℓ data and low- ℓ data (hereafter Planck data) using MCMC analysis [41]. Throughout our analyses, we have considered massless neutrinos which changes the values of the parameters slightly compared to the values obtained in ref. [7]. Since A_s and n_s have the same origin in the early universe, we fix the priors on these quantities from the Planck parameter estimation which gives $\ln(10^{10} \times A_s) = 3.072 \pm 0.027$ and $n_s = 0.9681 \pm 0.0058$.

In the next step, we find the best-fit values of σ_8 and other cosmological parameters without viscosity from LSS data which include Planck SZ survey [42], Planck lensing survey [43], Baryon Acoustic Oscillation data from BOSS [44, 45], South Pole Telescope (SPT) [46, 47] and CFHTLenS [48, 49] (hereafter LSS data). We keep τ_{reion} fixed at 0.070, since τ_{reion} does not have much effect on LSS. These LSS surveys altogether indicate a value of σ_8 to be $0.8034^{+0.0104}_{-0.0098}$ at 2- σ level whereas Planck CMB observations predicts it to be $0.8186^{+0.0180}_{-0.0216}$ at 2- σ level. Therefore, there exists a mismatch between these two observations which is evident in $\sigma_8 - \Omega_m$ plane shown in Fig. (4b) and Fig. (5b).

We proceed to the next step which is to obtain the best-fit value for the viscosity parameters $\tilde{\eta}$ and $\tilde{\zeta}$. In this step we keep A_s and n_s prior as obtained from the analysis of Planck data. The best-fit value for $\tilde{\eta}$ turns out to be $(2.30 \pm 0.58) \times 10^{-6}$ at 1- σ level, as shown in Fig. (4a) and the best-fit value of $\tilde{\zeta}$ turns out to be $(2.60 \pm 0.78) \times 10^{-6}$ at 1- σ level (Fig. (5a)).

Further, we set the values of viscosity parameters $\tilde{\eta}$ and $\tilde{\zeta}$ to their best-fit values obtained in the previous step. With these values we perform MCMC analysis for Planck data to obtain the statistical estimates of standard cosmological parameters $\{\Omega_b, \Omega_{\text{cdm}}, A_s, n_s, \Theta_{\text{MC}}, \tau_{\text{reion}}\}$ and the derived parameters H_0 and σ_8 . Finally, we perform similar analysis with LSS data by setting $\tilde{\eta}$ and $\tilde{\zeta}$ to their best-fit values. For this last step we keep the values of A_s and n_s obtained from the Planck as their prior.

As we have discussed in previous section, the viscosity in the cold dark matter reduces the power on small scales in matter power spectrum. As a consequence σ_8 shifts downward in $\sigma_8 - \Omega_m$ fitting plane for both the LSS and Planck CMB data. The result with viscosity shows a clear overlap of entire 1 σ region for $\sigma_8 - \omega_m$ which had earlier a 2 σ discordance (Fig. (4b) and Fig. (5b)).

4 Resolving $H_0 - \Omega_m$ tension

Measurements of the value of Hubble parameter are done in two different ways. One is the direct measurement from type-IA supernova and another one is the indirect estimation through LSS and CMB observations. From LSS observations H_0 is estimated as the required damping term in the growth of the over-densities, while from CMB observations H_0 is inferred from the scale Θ_{MC} of baryon acoustic oscillation.

The tension between the direct and indirect measurements is well known in the literature [50]. However, there was no disagreement between indirect measurements until the advent of Planck data. The WMAP 7 year result [51] has given such values of $H_0 - \Omega_m$ which can accommodate the LSS results. On the other hand, MCMC analysis done with Planck data, as described in the previous section shows some tension with LSS result obtained similarly with the Planck prior set on $\{A_s, n_s, \tau_{\text{reion}}\}$. Planck analysis gives the value of H_0 to be 67.91 ± 0.89 with $\Omega_m = 0.305 \pm 0.012$ where as the best-fitted value for H_0 turns out to be

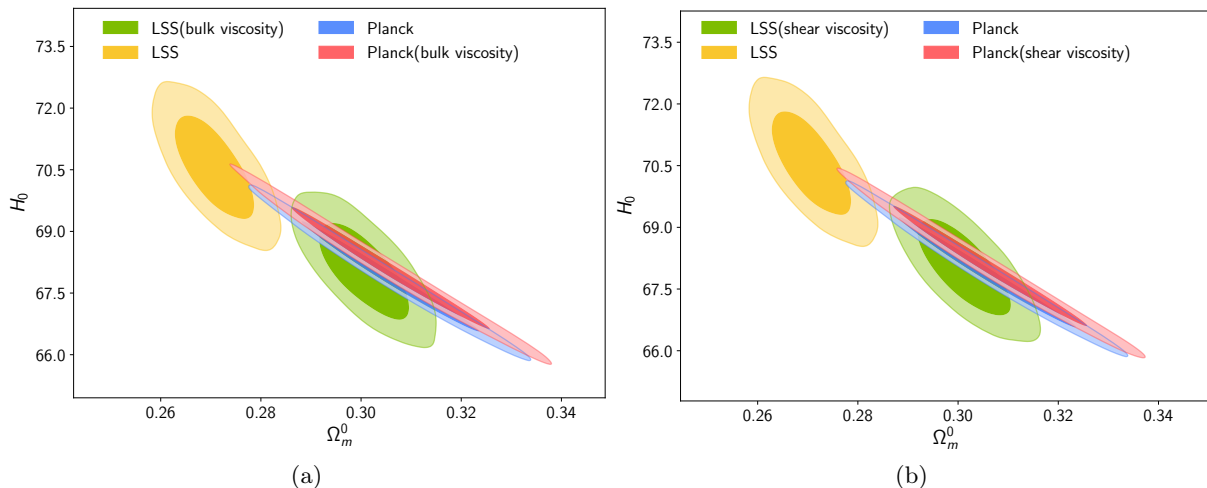


Figure 6: Bestfit parameter range for $H_0 - \Omega_m$ shows a clear discordance in 1σ level. This discordance gets resolved by introduction of (a) bulk viscosity or (b) shear viscosity in the CDM.

70.58 ± 0.83 and Ω_m is 0.270 ± 0.005 for LSS data at 1σ level. We see that there is clear discordance between these best-fit parameter regions in Fig. (6a) and Fig. (6b).

In viscous cosmology both Hubble and viscosities play similar kind of role. Hubble acts as an over-all damping term in eq. (2.17) and $\tilde{\eta}$, $\tilde{\zeta}$ go with scale dependent damping terms. Therefore on small scales viscosity compensates the effect of Hubble reducing the value of H_0 . On the other hand, the value of H_0 estimated from CMB does not get affected much as it is inferred from the acoustic scale Θ_{MC} . The role of viscosity in changing Ω_m^0 is not straightforward. However, it can be understood from eq. (2.17) and eq. (2.23) that Ω_{cdm} or Ω_{cdm}^0 comes in the denominator in the term with viscous parameters. Therefore, introduction of viscosity drags the value of Ω_{cdm}^0 towards higher values to compensate the effect of viscous term.

The MCMC analysis done in four steps, which had been described in last section, shows these shifts in $H_0 - \Omega_m^0$ plane. This shift ensures that the discordance between LSS and CMB observations disappear.

5 Planck-LSS combined viscous-cosmological parameters

We have seen that bulk and shear viscosity removes the tension between Planck and LSS observations. Therefore, we proceed to do a joint MCMC analysis using these two data sets. We keep bulk and shear viscosity parameters, $\tilde{\zeta}$ and $\tilde{\eta}$, varying to find the best-fit value for them; then in two different analyses, we kept one of the viscosity parameters to be zero to get the best-fit value of other. Since bulk and shear viscosities play almost similar role the best-fit value of shear(bulk) in the absence of bulk(shear) viscosity is different than that of the combined analysis.

We do not find any significant change in all the cosmological parameters from the Planck-fitted results. The only significant shift is visible in the derived parameter σ_8 which settles down to a lower value than the Planck-fitted value. The value of the newly fitted parameters

Parameter	1- σ value	2- σ value
Cosmological parameters		
$\Omega_b h^2$	0.0222 ± 0.0002	0.0222 ± 0.0004
$\Omega_{\text{cdm}} h^2$	0.1185 ± 0.0012	$0.1185^{+0.0024}_{-0.0024}$
$100\Theta_{\text{MC}}$	1.04212 ± 0.00039	$1.04212^{+0.00076}_{-0.00077}$
$\ln(10^{10} A_s)$	3.070 ± 0.023	$3.070^{+0.044}_{-0.045}$
n_s	0.9674 ± 0.0043	$0.9674^{+0.0086}_{-0.0084}$
τ_{reion}	0.069 ± 0.012	$0.069^{+0.023}_{-0.024}$
Viscosity parameters		
$\tilde{\eta}$	$1.20^{+0.40}_{-1.00} \times 10^{-6}$	$1.20^{+1.00}_{-1.00} \times 10^{-6}$
$\tilde{\zeta}$	$1.32^{+0.50}_{-1.00} \times 10^{-6}$	$1.32^{+2.00}_{-1.00} \times 10^{-6}$
In absence of bulk viscosity		
$\tilde{\eta}$	$2.29^{+0.50}_{-0.60} \times 10^{-6}$	$2.29^{+1.00}_{-1.00} \times 10^{-6}$
In absence of shear viscosity		
$\tilde{\zeta}$	$2.46^{+0.50}_{-0.60} \times 10^{-6}$	$2.46^{+1.00}_{-1.00} \times 10^{-6}$
Derived parameters		
H_0 (Km/sec/Mpc)	68.39 ± 0.56	$68.4^{+1.1}_{-1.1}$
σ_8	0.754 ± 0.011	$0.754^{+0.022}_{-0.021}$

Table 1: Best-fit values of cosmological parameters along with the viscosity parameters and the derived parameters for viscous cosmology are shown here. These values are obtained from Planck-LSS joint analyses in the presence of both bulk and shear viscosities. These values remain almost unchanged for the analyses with only one type of viscosity.

are shown in table-1. The best fit value of σ_8 obtained from the analysis done with either type of viscosity does not change significantly from that of the bulk-shear combined analysis.

6 Discussion and Conclusion

Through out this paper we have discussed the effect of two different viscosities on large scale structure formations and CMB. We have found that either of the two viscosities or their combination affects the growth of linear overdensity which in turn changes the matter power spectrum at small length scales. Motivated by this, we move on to quantify the amount of viscosity supported by cosmological observations. Therefore, we consider the viscosity coefficients as model parameters and perform MCMC analysis with Planck and LSS data. In the analyses with LSS data, the values of amplitude of primordial perturbations and scalar spectral index is set to be equal to the value obtained from Planck CMB analysis. We find that some amount of viscosity is preferred by LSS observations. Most interestingly this bestfit value of viscosity resolves the conflict between Planck CMB and LSS observations, both in $\sigma_8 - \Omega_m^0$ plane and $H_0 - \Omega_m^0$ plane, simultaneously. It is interesting to note that the value of H_0 inferred from Planck does not change significantly due to the viscosities, while the same obtained from LSS changes significantly. This is due to the following reasons: H_0 is obtained from the baryon acoustic oscillation scale and depends on the value of Ω_m^0 [52]. The LSS experiments constrain σ_8 and Ω_m^0 jointly [48] which gives a scope to accommodate lower σ_8 by increasing Ω_m^0 . However, in the case of Planck data, σ_8 is a derived parameter which comes down to a lower value, due to inclusion of viscosity, without affecting Ω_m^0 . Therefore, in the

case of σ_8 , both Planck and LSS fitted values change on inclusion of viscosities, but for the H_0 only LSS value gets affected.

We find that the required value of bulk and shear viscosity parameters ($\tilde{\zeta}$ and $\tilde{\eta}$), as obtained from MCMC analyses, are of same order ($\mathcal{O}(10^{-6})$) and have similar effects. It is almost impossible to distinguish the effects arising from these two viscosities. The best-fit values for commonly used viscosity parameters η and $\zeta \sim 3 \times 10^2$ Pa.sec .

The origin of these viscosities can have different sources. The fundamental viscosity generated by the self-interaction between the dark matter particles might be one source. Another source can be the large-scale integrated effect of the small scale non-linear gravitational phenomenon [28]. One might also attribute this kind of viscosity to the corrections in the gravity sector of the Einstein-Hilbert action [53].

The fundamental viscosity generated by the self-interaction between the dark matter particles can be written in terms of the cross-section to mass ratio, σ/m [54]. However it depends on the details of the decoupling history of dark matter. So the relation between the viscous coefficients η , ζ and σ/m is model dependent. The observational bound from bullet-cluster [55] on the cross-section to mass ratio σ/m for self-interacting dark matter is $\sigma/m \leq 1.2 \text{ cm}^2/\text{g}$. This gives the value of mean free path of the dark matter particle greater than the horizon size at present day. Therefore a hydrodynamic description might not be valid during late time, but it can work in the past when mean free path was within the horizon.

Previous attempts in the literature to remove the tension between LSS and Planck CMB for σ_8 and H_0 either include sterile neutrinos or exotic interaction in dark sectors. However, these attempts fails to resolve both the discordances simultaneously. We, on the other hand, did not introduce any extra matter component to the Λ CDM cosmology. Moreover, we solve the two issues of σ_8 and H_0 with introduction of only one parameter, either bulk or shear viscosity. The origin of these dissipative effects requires a thorough investigation of the properties of dark matter in future.

Acknowledgement:

We would like to thank Thejs Brinckmann and Miguel Zumalacàrregui for their help related to MontePython.

References

- [1] F. Zwicky, *Die Rotverschiebung von extragalaktischen Nebeln*, *Helv. Phys. Acta* **6** (1933) 110–127. [Gen. Rel. Grav.41,207(2009)].
- [2] V. C. Rubin and W. K. Ford, Jr., *Rotation of the Andromeda Nebula from a Spectroscopic Survey of Emission Regions*, *Astrophys. J.* **159** (1970) 379–403.
- [3] **Supernova Cosmology Project** Collaboration, S. Perlmutter et al., *Measurements of the cosmological parameters Omega and Lambda from the first 7 supernovae at $z >= 0.35$* , *Astrophys. J.* **483** (1997) 565, [[astro-ph/9608192](#)].
- [4] **Supernova Cosmology Project** Collaboration, S. Perlmutter et al., *Measurements of Omega and Lambda from 42 high redshift supernovae*, *Astrophys. J.* **517** (1999) 565–586, [[astro-ph/9812133](#)].
- [5] **Supernova Search Team** Collaboration, A. G. Riess et al., *Observational evidence from supernovae for an accelerating universe and a cosmological constant*, *Astron. J.* **116** (1998) 1009–1038, [[astro-ph/9805201](#)].

- [6] **WMAP** Collaboration, G. Hinshaw et al., *Nine-Year Wilkinson Microwave Anisotropy Probe (WMAP) Observations: Cosmological Parameter Results*, *Astrophys. J. Suppl.* **208** (2013) 19, [[arXiv:1212.5226](#)].
- [7] **Planck** Collaboration, P. A. R. Ade et al., *Planck 2015 results. XIII. Cosmological parameters*, *Astron. Astrophys.* **594** (2016) A13, [[arXiv:1502.01589](#)].
- [8] **DES** Collaboration, M. A. Troxel et al., *Dark Energy Survey Year 1 Results: Cosmological Constraints from Cosmic Shear*, [arXiv:1708.01538](#).
- [9] **HST** Collaboration, W. L. Freedman et al., *Final results from the Hubble Space Telescope key project to measure the Hubble constant*, *Astrophys. J.* **553** (2001) 47–72, [[astro-ph/0012376](#)].
- [10] A. Vikhlinin et al., *Chandra Cluster Cosmology Project III: Cosmological Parameter Constraints*, *Astrophys. J.* **692** (2009) 1060–1074, [[arXiv:0812.2720](#)].
- [11] E. Macaulay, I. K. Wehus, and H. K. Eriksen, *Lower Growth Rate from Recent Redshift Space Distortion Measurements than Expected from Planck*, *Phys. Rev. Lett.* **111** (2013), no. 16 161301, [[arXiv:1303.6583](#)].
- [12] R. A. Battye, T. Charnock, and A. Moss, *Tension between the power spectrum of density perturbations measured on large and small scales*, *Phys. Rev.* **D91** (2015), no. 10 103508, [[arXiv:1409.2769](#)].
- [13] N. MacCrann, J. Zuntz, S. Bridle, B. Jain, and M. R. Becker, *Cosmic Discordance: Are Planck CMB and CFHTLenS weak lensing measurements out of tune?*, *Mon. Not. Roy. Astron. Soc.* **451** (2015), no. 3 2877–2888, [[arXiv:1408.4742](#)].
- [14] **SPT** Collaboration, K. Aylor et al., *A Comparison of Cosmological Parameters Determined from CMB Temperature Power Spectra from the South Pole Telescope and the Planck Satellite*, [arXiv:1706.10286](#).
- [15] M. Raveri, *Are cosmological data sets consistent with each other within the Λ cold dark matter model?*, *Phys. Rev.* **D93** (2016), no. 4 043522, [[arXiv:1510.00688](#)].
- [16] W. Lin and M. Ishak, *Cosmological discordances: A new measure, marginalization effects, and application to geometry versus growth current data sets*, *Phys. Rev.* **D96** (2017), no. 2 023532, [[arXiv:1705.05303](#)].
- [17] **DES** Collaboration, T. M. C. Abbott et al., *Dark Energy Survey Year 1 Results: Cosmological Constraints from Galaxy Clustering and Weak Lensing*, [arXiv:1708.01530](#).
- [18] A. Poursidou and T. Tram, *Reconciling CMB and structure growth measurements with dark energy interactions*, *Phys. Rev.* **D94** (2016), no. 4 043518, [[arXiv:1604.04222](#)].
- [19] V. Salvatelli, N. Said, M. Bruni, A. Melchiorri, and D. Wands, *Indications of a late-time interaction in the dark sector*, *Phys. Rev. Lett.* **113** (2014), no. 18 181301, [[arXiv:1406.7297](#)].
- [20] W. Yang and L. Xu, *Cosmological constraints on interacting dark energy with redshift-space distortion after Planck data*, *Phys. Rev.* **D89** (2014), no. 8 083517, [[arXiv:1401.1286](#)].
- [21] P. Ko and Y. Tang, *Light dark photon and fermionic dark radiation for the Hubble constant and the structure formation*, *Phys. Lett.* **B762** (2016) 462–466, [[arXiv:1608.01083](#)].
- [22] P. Ko and Y. Tang, *Residual Non-Abelian Dark Matter and Dark Radiation*, *Phys. Lett.* **B768** (2017) 12–17, [[arXiv:1609.02307](#)].
- [23] P. Ko, N. Nagata, and Y. Tang, *Hidden Charged Dark Matter and Chiral Dark Radiation*, [arXiv:1706.05605](#).
- [24] M. Wyman, D. H. Rudd, R. A. Vanderveld, and W. Hu, *Neutrinos Help Reconcile Planck Measurements with the Local Universe*, *Phys. Rev. Lett.* **112** (2014), no. 5 051302, [[arXiv:1307.7715](#)].

- [25] R. A. Battye and A. Moss, *Evidence for Massive Neutrinos from Cosmic Microwave Background and Lensing Observations*, *Phys. Rev. Lett.* **112** (2014), no. 5 051303, [[arXiv:1308.5870](#)].
- [26] S. Riemer-Sørensen, D. Parkinson, and T. M. Davis, *Combining Planck data with large scale structure information gives a strong neutrino mass constraint*, *Phys. Rev.* **D89** (2014) 103505, [[arXiv:1306.4153](#)].
- [27] S. Camera, M. Martinelli, and D. Bertacca, *Easing Tensions with Quartessence*, [[arXiv:1704.06277](#)].
- [28] D. Blas, S. Floerchinger, M. Garny, N. Tetradis, and U. A. Wiedemann, *Large scale structure from viscous dark matter*, *JCAP* **1511** (2015) 049, [[arXiv:1507.06665](#)].
- [29] H. Velten, T. R. P. Caramãis, J. C. Fabris, L. Casarini, and R. C. Batista, *Structure formation in a Λ viscous CDM universe*, *Phys. Rev.* **D90** (2014), no. 12 123526, [[arXiv:1410.3066](#)].
- [30] D. B. Thomas, M. Kopp, and C. Skordis, *Constraining the Properties of Dark Matter with Observations of the Cosmic Microwave Background*, *Astrophys. J.* **830** (2016), no. 2 155, [[arXiv:1601.05097](#)].
- [31] C. M. S. Barbosa, H. Velten, J. C. Fabris, and R. O. Ramos, *Assessing the impact of bulk and shear viscosities on large scale structure formation*, *Phys. Rev.* **D96** (2017), no. 2 023527, [[arXiv:1702.07040](#)].
- [32] M. Kunz, S. Nesseris, and I. Sawicki, *Constraints on dark-matter properties from large-scale structure*, *Phys. Rev.* **D94** (2016), no. 2 023510, [[arXiv:1604.05701](#)].
- [33] I. Brevik, Å. Grøn, J. de Haro, S. D. Odintsov, and E. N. Saridakis, *Viscous Cosmology for Early- and Late-Time Universe*, [[arXiv:1706.02543](#)].
- [34] J. M. Bardeen, *Gauge Invariant Cosmological Perturbations*, *Phys. Rev.* **D22** (1980) 1882–1905.
- [35] J. R. Bond and G. Efstathiou, *Cosmic background radiation anisotropies in universes dominated by nonbaryonic dark matter*, *Astrophys. J.* **285** (1984) L45–L48.
- [36] H. Kodama and M. Sasaki, *Cosmological Perturbation Theory*, *Prog. Theor. Phys. Suppl.* **78** (1984) 1–166.
- [37] C.-P. Ma and E. Bertschinger, *Cosmological perturbation theory in the synchronous and conformal Newtonian gauges*, *Astrophys. J.* **455** (1995) 7–25, [[astro-ph/9506072](#)].
- [38] S. Weinberg, *Gravitation and Cosmology*, p.p:55-57. John Wiley and Sons, New York, 1972.
- [39] J. Lesgourgues, *The Cosmic Linear Anisotropy Solving System (CLASS) I: Overview*, [[arXiv:1104.2932](#)].
- [40] D. Blas, J. Lesgourgues, and T. Tram, *The Cosmic Linear Anisotropy Solving System (CLASS) II: Approximation schemes*, *JCAP* **1107** (2011) 034, [[arXiv:1104.2933](#)].
- [41] B. Audren, J. Lesgourgues, K. Benabed, and S. Prunet, *Conservative Constraints on Early Cosmology: an illustration of the Monte Python cosmological parameter inference code*, *JCAP* **1302** (2013) 001, [[arXiv:1210.7183](#)].
- [42] **Planck** Collaboration, P. A. R. Ade et al., *Planck 2013 results. XX. Cosmology from Sunyaev-Zeldovich cluster counts*, *Astron. Astrophys.* **571** (2014) A20, [[arXiv:1303.5080](#)].
- [43] **Planck** Collaboration, P. A. R. Ade et al., *Planck 2013 results. XVII. Gravitational lensing by large-scale structure*, *Astron. Astrophys.* **571** (2014) A17, [[arXiv:1303.5077](#)].
- [44] **BOSS** Collaboration, L. Anderson et al., *The clustering of galaxies in the SDSS-III Baryon Oscillation Spectroscopic Survey: baryon acoustic oscillations in the Data Releases 10 and 11 Galaxy samples*, *Mon. Not. Roy. Astron. Soc.* **441** (2014), no. 1 24–62, [[arXiv:1312.4877](#)].

- [45] **BOSS** Collaboration, A. Font-Ribera et al., *Quasar-Lyman α Forest Cross-Correlation from BOSS DR11 : Baryon Acoustic Oscillations*, *JCAP* **1405** (2014) 027, [[arXiv:1311.1767](#)].
- [46] K. K. Schaffer et al., *The First Public Release of South Pole Telescope Data: Maps of a 95-square-degree Field from 2008 Observations*, *Astrophys. J.* **743** (2011) 90, [[arXiv:1111.7245](#)].
- [47] A. van Engelen et al., *A measurement of gravitational lensing of the microwave background using South Pole Telescope data*, *Astrophys. J.* **756** (2012) 142, [[arXiv:1202.0546](#)].
- [48] M. Kilbinger et al., *CFHTLenS: Combined probe cosmological model comparison using 2D weak gravitational lensing*, *Mon. Not. Roy. Astron. Soc.* **430** (2013) 2200–2220, [[arXiv:1212.3338](#)].
- [49] C. Heymans et al., *CFHTLenS tomographic weak lensing cosmological parameter constraints: Mitigating the impact of intrinsic galaxy alignments*, *Mon. Not. Roy. Astron. Soc.* **432** (2013) 2433, [[arXiv:1303.1808](#)].
- [50] L. Verde, P. Protopapas, and R. Jimenez, *The expansion rate of the intermediate Universe in light of Planck*, *Phys. Dark Univ.* **5-6** (2014) 307–314, [[arXiv:1403.2181](#)].
- [51] **WMAP** Collaboration, E. Komatsu et al., *Seven-Year Wilkinson Microwave Anisotropy Probe (WMAP) Observations: Cosmological Interpretation*, *Astrophys. J. Suppl.* **192** (2011) 18, [[arXiv:1001.4538](#)].
- [52] B. A. Bassett and R. Hlozek, *Baryon Acoustic Oscillations*, [[arXiv:0910.5224](#)].
- [53] A. Abebe, M. Abdelwahab, A. de la Cruz-Dombriz, and P. K. S. Dunsby, *Covariant gauge-invariant perturbations in multifluid $f(R)$ gravity*, *Class. Quant. Grav.* **29** (2012) 135011, [[arXiv:1110.1191](#)].
- [54] S. Gavin, *TRANSPORT COEFFICIENTS IN ULTRARELATIVISTIC HEAVY ION COLLISIONS*, *Nucl. Phys.* **A435** (1985) 826–843.
- [55] F. Kahlhoefer, K. Schmidt-Hoberg, M. T. Frandsen, and S. Sarkar, *Colliding clusters and dark matter self-interactions*, *Mon. Not. Roy. Astron. Soc.* **437** (2014), no. 3 2865–2881, [[arXiv:1308.3419](#)].